Research

Author for correspondence:
Balasubramanian Kandasubramanian
e-mail: meetkbs@gmail.com

Functionalized non-woven surfaces for combating the spread of the COVID-19 pandemic

Nikhil Avinash Patil[1], Prakash Macchindra Gore[1,2], Dhivya Shanmugrajan[3], Harshal Patil[4], Mahesh Kudav[4] and Balasubramanian Kandasubramanian[1,2]

[1]Nanofibre and Nano Surface Texturing Laboratory, Department of Metallurgical and Materials Engineering, Defence Institute of Advanced Technology, Ministry of Defence, Girinagar, Pune, Maharashtra 411025, India
[2]Institute for Frontier Materials, Deakin University, Waurn Ponds Campus, Geelong 3216, Victoria, Australia
[3]Department of Life Sciences, Altem Technologies, Platinum Partner of Dassault Systemes, Bangalore 560095, Karnataka, India
[4]Venus Safety and Health Pvt Ltd, New Mumbai 410208, Maharashtra, India

PMG, 0000-0002-3993-8763; BK, 0000-0003-4257-8807

The worldwide outbreak of SARS-CoV-2 infection has necessitated mandatory use of face masks, personal protective equipment and intake of a healthy diet for immunity boosting. As per WHO's recommendation, continuous use of masks has been proven effective in decreasing the SARS-CoV-2 infection rate. The present study reports on the bacterial filtration efficacy (BFE) of a novel 4-ply functionalized non-woven face mask. We synthesized a polypropylene-based fabric with inner layers of melt-blown fine fibres coated with polylactic acid and immune-boosting herbal phytochemicals. Experimental studies on the synthesized face mask demonstrated a BFE of greater than 99% against *Staphylococcus aureus* (a bacterium species frequently found in mammalian respiratory tract). A thorough computational analysis using LibDock algorithm demonstrated an effective docking performance of herbal phytochemicals against harmful virus structures. More importantly, the face mask also showed sufficient and stable breathability as per regulatory standards. A breathing resistance of 30 Pa at an aerosol flow rate of 30 l h^{-1} was reported under standard temperature and pressure conditions, indicating a high potential for real-world applications.

1. Introduction

An outburst of contagious SARS-CoV-2 pandemic resulted in spread of infection waves, radically affecting health conditions of people across the world and leaving behind long-term respiratory health effects [1]. As per WHO recommendations, the spread of viral infections can be restricted with continuous use of protective masks and personal protective equipment suits [2], since the viral infections mainly occur through aerosol droplets in air which directly attack the human respiratory system [3,4]. Non-woven face masks are widely used due to tailorable fibre diameters for various layers, filtration of aerosol particles, sterility, low production costs, shorter production cycles, leverage to incorporate antibacterial materials and higher flexibility [5–9]. Considering various non-woven fabric manufacturing techniques, a combination of melt-blown and spun-bonded non-woven fabrics shows stable air filtration properties for biomedical applications [10].

Tellier *et al.* [11] reported that the spread of virus occurs rapidly through respiratory tract due to the presence of aerosol particles in the air. However, the transport of these infections aerosols can be mitigated by applying a barrier prior to their entry to the respiratory tract [12]. Hence, continuous use of face masks became an important precautionary measure for protection against deadly infectious viruses [13]. This necessitated modifications in the morphology of the protective masks to achieve a bacterial filtration efficacy (BFE) of

THE ROYAL SOCIETY
PUBLISHING

99% (or higher), leading to development of the multiple-layered structure exhibiting ameliorated filtration performance [14]. In a recent study [15], we demonstrated that the incorporation of polylactic acid (PLA) and traditional Indian phytochemical-based filtration layers in cotton-based face masks renders an immuno-boosting effect to the mask wearer and enhances BFE of the protective mask [16]. It has been identified that factors such as the surface area of aerosol particles and surface wettability of non-woven surfaces play a key role in the transmission of virus from the environment into human body [17]. It has also been established that hydrophobic surfaces restrict the passage of aerosol particles through the non-woven surfaces, whereas hydrophilic surfaces permit absorption of aerosol particles [18].

Based on the investigations of Ayurveda, phytochemicals or oil extracts of spices demonstrate inflammatory response to counter the biological harmful viral infections [19–21]. In a recent study, Xiong *et al.* [22] reported the effectiveness of Chinese herbal-based extracts against the harmful SARS-CoV-2 viral infection. It was also observed that glucocorticoids-based drug treatments for SARS-CoV-2 infections showed decline in the mechanical ventilation and mortality ratio among the affected patients when compared with standard care protocols [23]. Bartonkova *et al.* [24] reported the effective performance of herbal extracts on glucocorticoid based receptors, which exhibited anti-hypertensive, anti-fungal, anti-microbial and anti-inflammatory properties, boosting the immune response against the harmful viral infections. Similarly, Kumar *et al.* [25] demonstrated non-mutagenic, non-toxic, non-irritant and biodegradable performance of organic compounds at a lower concentration for plant-based herbal phytochemical oils.

The present study reports on the BFE of a functionalized 4-ply non-woven face mask and its immune-boosting characteristics. The functionalization of non-woven substrates was achieved by spray coating of polymeric layer over the melt-spun non-woven filter media. This was followed by performing a thorough computational analysis using LibDock algorithm to analyse the docking performance of herbal phytochemicals against infectious virus structures. Field-emission scanning electron microscopy (FE-SEM) was performed on the functionalized fibres to examine the compact microstructure and to identify the impact of fibre augmentation on aerosol penetration efficacy. Subsequently, the surface wetting analysis of the spray-coated non-woven layer was investigated using a contact angle goniometer. Finally, the developed face mask was tested against *Staphylococcus aureus* (ATCC 6538, an international standard testing strain for disinfectants) to examine the BFE of the augmented 4-ply mask. The results of this study are therefore expected to be of high value for the scientific and engineering community.

2. Fabrication of the mask material and surface morphology

A four-ply non-woven breathable face mask is shown in figure 1*a*,*b*. The hydrophobic outer layer consists of non-woven spun-bonded polypropylene fibres exhibiting a uniformly distributed diameter of 15.87 ± 0.5 µm figure 2*b*, which renders a compact close-packed structure, and improved surface area for restricting the transmission of aerosol droplets (figure 2*a–f*) [26,27]. Finely distributed non-woven fibres (less than 17 µm), and thickness of 0.57 mm, further support in
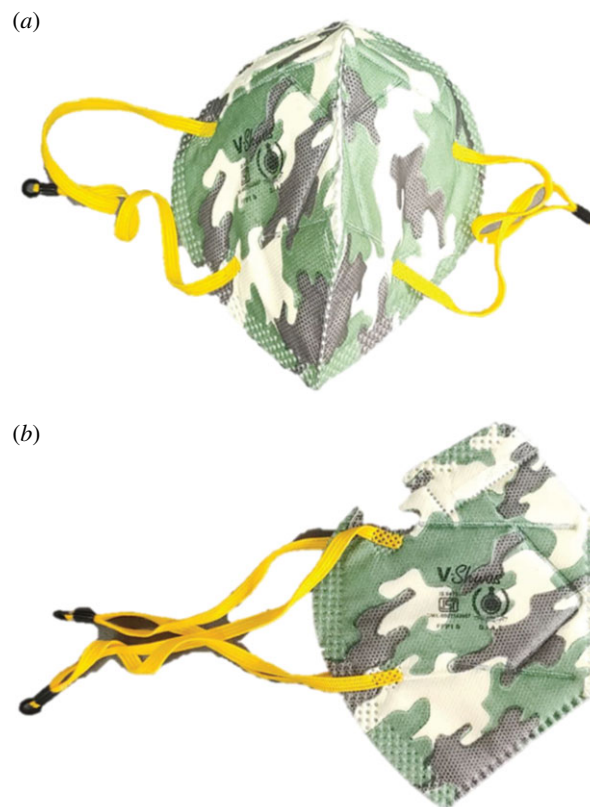

Figure 1. Marketed product image of Aushadatara face mask.

obstructing the entry of aerosol particles (50–500 nm) for improved filtration efficacy [28]. The second layer consists of non-woven melt-blown fine fibres exhibiting a diameter of 613.3 nm (figure 2*d*), which was used as filter media in the face mask. As depicted in figure 2*d*, a dense structure of uniformly distributed melt-blown fibres could potentially aid in enhancing the bacterial and viral filtration performance of the face mask [29,30]. Third layer of the mask was fabricated using spray coating of herbal phytochemical encapsulated PLA. This was performed to enhance the immune-boosting characteristics via inhalation to the mask wearer [31–33]. Mean thicknesses of the outer to inner layer (four layers) of the mask were found to be 0.28 ± 0.01 mm, 0.13 ± 0.01 mm, 0.13 ± 0.01 mm and 0.21 ± 0.01 mm, respectively. The thickness of entire face mask was found to be 1.25 ± 0.01 mm.

3. Bacterial filtration efficiency and breathing resistance

It is established that spun-bonded polypropylene fabric layers facilitate the removal of large aerosol particles and particulate matter (PM), whereas the lower sized molecules get trapped in compact melt-blown polyester-based filter media and PLA/herbal-extract spray-coated layer [34]. FE-SEM micrographs (figure 2*a–f*) demonstrate densely packed fibre morphology of the non-woven filter layer, with uniform fibre diameter distribution. It has been established that a uniformly distributed fibre diameter facilitates narrow pore sites for trapping the aerosol and PM particles and enhances the active surface area [35,36]. Thus, the high BFE of the mask's filter media can be linked to the fibre diameters. The stable air filtration ability of the filter layer was attributed to the adsorption phenomena of the small sized impurities as per
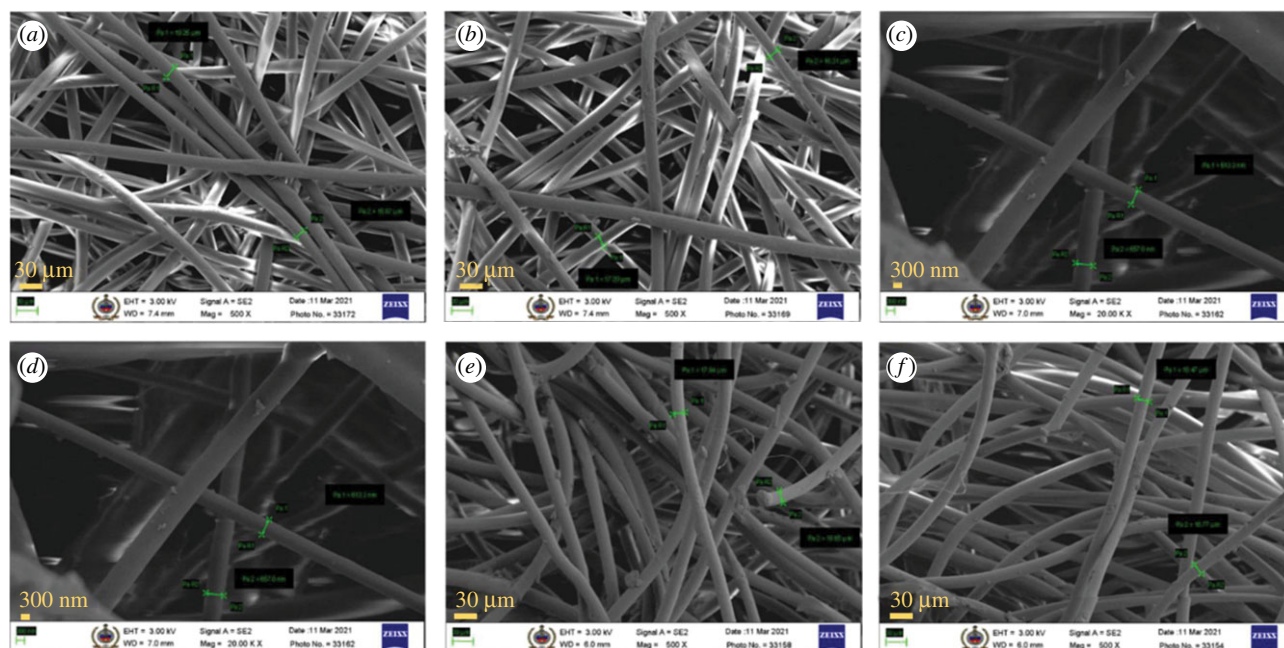
Figure 2. FE-SEM micrographs of the face mask sample. (*a*) Washed sample of spun-bonded outermost layer of face mask, (*b*) unwashed sample of outermost layer of face mask, (*c*) washed sample of melt-blown filter media, (*d*) unwashed sample of melt-blown filter media, (*e*) washed sample of PLA spray-coated layer and (*f*) unwashed sample of PLA spray-coated layer.

the following five mechanisms: (i) gravity effect, (ii) inertial impaction, (iii) electrostatic effect, (iv) interception and (v) Brownian diffusion [37]. These mechanisms might show variations in filtration capabilities of fibre layers, whereas the overall filtration performance of protective mask was determined by the collective performance of several mechanisms considering the particle size of particulate impurities in atmosphere [38,39]. The addition of herbal-extract phytochemicals in layered structure of protective mask facilitated enhanced filtration efficiency and also it did not affect the differential pressure, thereby improving the overall bacterial protection against viral infections and harmful pathogens [40]. In the present investigation, four-layered non-woven protective mask with herbal phytochemicals demonstrated BFE of 99.65% against *Staphylococcus aureus* bacteria (as per AATCC 6538 standard), with an average bacterial count as 10 and average bacterial count for positive control as 2900. Note that the BFE of the mask without herbal phytochemicals was found to be 95% as per the above-mentioned test standards. Thus, it was observed that the inclusion of herbal phytochemicals helped in enhancing the BFE of the face mask. This advancement was further acknowledged by the regulatory agencies. The developed non-woven protective mask passed European Commission's regulatory certification (Certificate No. 17020). The face mask is currently registered with a trademark name of Aushadatara Trademark No. 4595855.

The fibre diameter distribution analysis is presented in figure 3*a*–*f*, and its main results are tabulated in table 1. As depicted, it was found that the outer layer, and spray-coated layers (both washed and unwashed) exhibited constant fibre diameter in the range of 17–18 µm, whereas the inner melt-blown layer (washed and unwashed) revealed fine fibre diameter ranging from 0.731 µm to 1.1 µm. Fibre distribution analysis showed that all layers possess uniform fibre diameters, thereby confirming the consistency of face mask fabrication process.

As per Indian IS 9734:2002 standard, the protective mask demonstrated low differential pressure and breathing resistance across layers of protective mask. Details on the breathing resistance of the face mask are reported in table 2.

4. Computational analysis and immune-boosting characteristics

The utilization of herbal phytochemicals was beneficial for imparting antibacterial characteristics in the developed mask. An investigation by Ali *et al.* [41] demonstrated the antibacterial performance of *Azadirachta indica* (*A. indica*) against bacteria by developing an inhibition zone of 14.5 mm, which was attributed to the presence of nearly 140 biologically active constituents. They argued that the existence of several bioactive compounds like triterpinoids, alkaloids, asteroids, reducing sugars, flavonoids, tannins, phenolic compounds and sesquiterpene lactones collectively imparted antibacterial activity [41]. Consequently, *A. indica* has been used in treating various skin infections, dental problems and skin inflammations [41]. Similarly, Subramani *et al.* [42] reported cotton fabric functionalized with *A. indica* nanoparticles which demonstrated antibacterial activity with zones of inhibition of 34 mm and 31.58 mm against *S. aureus* and *E. coli*, respectively. They claimed that *A. indica*-coated cotton fabric showed nearly 47% and 45% bacterial reduction efficacy towards *E. coli* and *S. aureus*, respectively. Yadav & Kandasubramanian [9] showed that *A. india* engineered polyvinyl alcohol membrane exhibiting rough texture and cross-linked with egg albumin demonstrated zones of inhibition of 2.6 cm and 2.8 cm towards *S. aureus* and *E. coli*, respectively. In similar study Yadav & Kandasubramanian [21] reported antibacterial nanocomposite prepared using *Syzygium aromaticum* and electrospun polyacrylonitrile (PAN) nanofibres, which revealed antibacterial performance with zones of inhibition of 1.8 cm and 2.8 cm
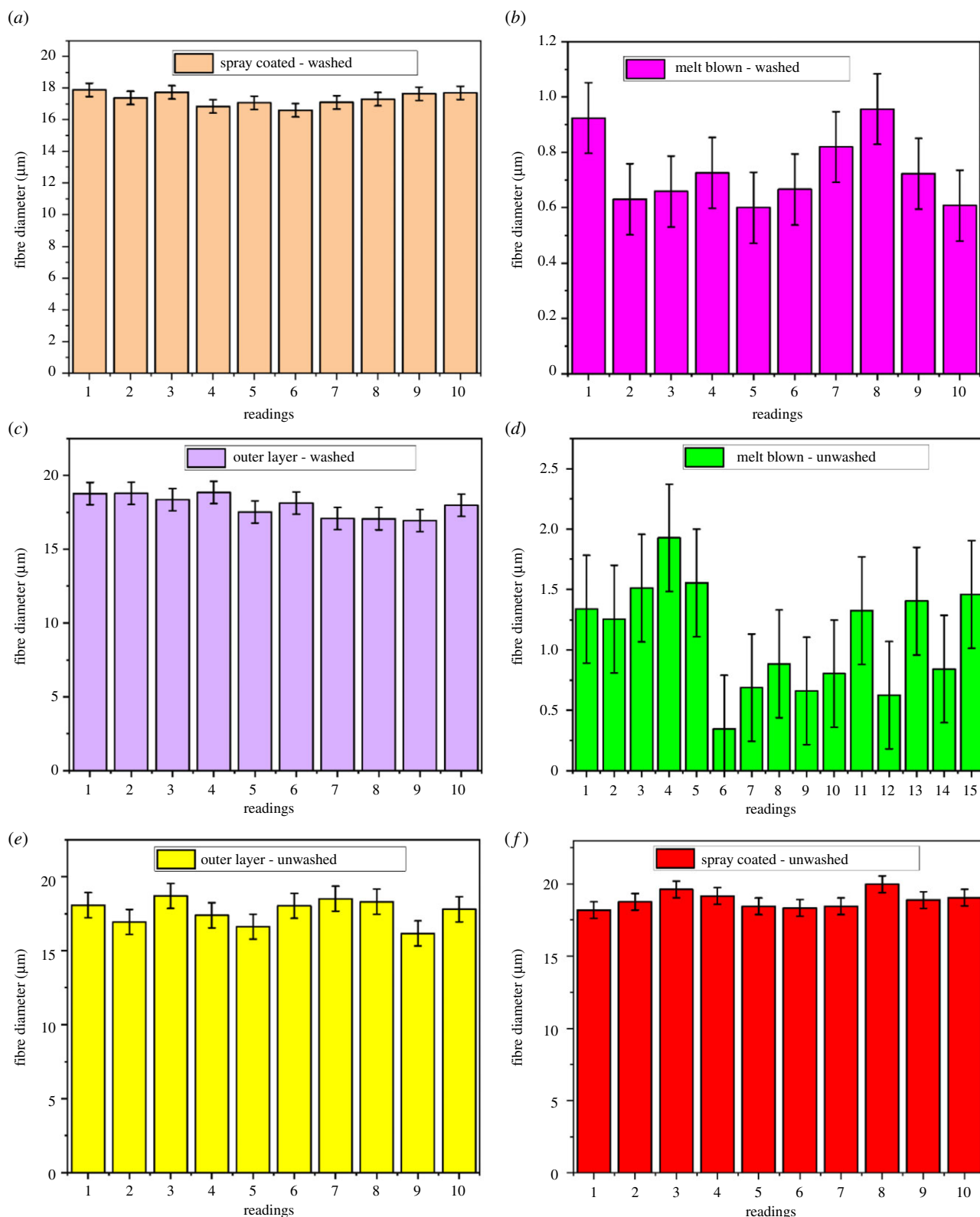
Figure 3. Fibre diameter distribution of (*a*) washed spray-coated layers, (*b*) washed melt-blown layers, (*c*) washed outer layers, (*d*) unwashed melt-blown layer, (*e*) unwashed outer layer and (*f*) unwashed spray-coated layer at a standard room temperature of $25 \pm 2°C$.

against *S. aureus* and *E. coli*, respectively, and cell viability of 100% as per standard NIH/3T3 test. In another study, Govindaraj *et al.* [43] reported *Curcuma longa* (*C. longa*) oil embedded PAN membrane films which exhibited antimicrobial activity against *S. aureus* and *E. coli* with zone of inhibition of 0.8 cm to 1 cm. They claimed that antibacterial efficacy of *C. longa* was attributed to the presence of pleiotropic polyphenolic curcumin (diferuloylmethane) element, which directly interacted with target molecules and therefore traditionally

used in therapeutic remediation. Verma & Balasubramanian [44] reported herbal *Lantana camara* oil-based PAN membrane films which demonstrated antibacterial resistance against *B. subtilis* and *E. coli* with zones of inhibition of 7–8 mm and 8–10 mm, respectively. They claimed that antibacterial performance of PAN membrane films was attributed to the collective presence of α-humulene compound (9.3%), germacrene-D compound (19.8%), bicyclogermacrene (11.7%) and E-caryophyllene compound (19.7%) in the *L. camara* oil which drive direct

Table 1. Fibre diameter uniformity analysis.

sample specimen	mean diameter (µm)	standard deviation (±)
outer layer unwashed	17.657	0.848
outer layer washed	17.948	0.754
spray-coated layer unwashed	18.885	0.577
spray-coated layer washed	17.327	0.421
melt-blown unwashed	1.108	0.444
melt-blown washed	0.731	0.128

Table 2. Average breathing resistance of face mask as per Indian IS9734:2002 standard.

activity	flow rate (litre per hour)	average breathing resistance (Pa)
inhalation	30	30
inhalation	95	110
exhalation	160	175

molecular interactions with targeted molecules [44]. Similarly, Balasubramanian & Kodam [45] reported herbal lavender oil functionalized PAN nanofibres which exhibited antibacterial resistance against *S. aureus* with *K. pneumoniae* with a zone of inhibition of 14–15 mm. Considering the results discussed in above-mentioned studies, herbal phytochemicals were found to be safe in lower concentration for immunity boosting, traditional home remedies and personal hygiene. Diffusion of these herbal phytochemicals in low concentration through fibre layers and subsequent inhalation helps in improving the immunity boosting, personal hygiene, and gives comfort feeling, e.g. Vicks inhalers, to the mask bearing person [46]. Computational analysis of the phytochemicals as per formulation (A) for countering protein-structured viral and bacterial targets is significant for predicting the performance of constituent phytochemicals for impeding the virus protein structure [47] (figure 4). Computational investigation of phytochemicals was performed with scoring function based on LibDock algorithm.

An *in silico* analysis predicted the performance of structural characteristics of phytochemicals and protein–ligand complex for countering multiple bacterial targets. Docking score determines the structural complementarity of phytochemicals for analysing the neutralizing characteristics of phytochemicals against protein structures. Neutralizing performance of phytochemicals is accredited to their excellent docking score and capacity to undertake an interaction for protein unfolding. Higher docking score of salanin, arachidic acid, stearic acid and palmitic acid to counter protein structure of SARS-2 virus was attributed to the existence of hydrogen bond acceptor and aliphatic chains as it amplifies hydrogen bonding within protein–ligand compound due to attraction between electron lone pair and acceptor positive charge [48]. Aliphatic structure leads to efficient spin of bonds for occupying the targeted binding location, thereby improving the docking performance of

constituent chemicals for countering the protein structure [48,49]. Neutralizing performance of stearic acid to counter the protein folding of H7N9 virus was enabled due to the presence of hydrogen bond acceptors. Similarly, the confined performance of *cis*-11-octadecanoic acid and arachidic acid to counter the protein structure of Dengue virus was attributed to the aliphatic structure of constituent herbal extracts, leading to an efficient-binding performance at targeted protein interface. Structural compatibility of salanin against influenza virus demonstrated an optimal docking score, resulting in improved binding of ligand structure against the protein-structured binding sites. Hindered performance of oleic acid and stearic acid was significant due to structural compatibility of constituent chemicals to counter hantavirus. Structural attributes of palmitic acid, stearic acid and oleic acid against hepatitis C virus demonstrated an enhanced docking score leading to improved binding of ligand molecules across the protein structures. The neutralizing performance of oleic acid and linoleic acid was significant for exhibiting structural compatibility against Ebola virus and herpes simplex virus. Computational analysis revealed antibacterial/microbial performance of ayurvedic phytochemicals to counter the protein-structured virus, for restricting the spread of viral and bacterial infections through COVID-19 pandemic.
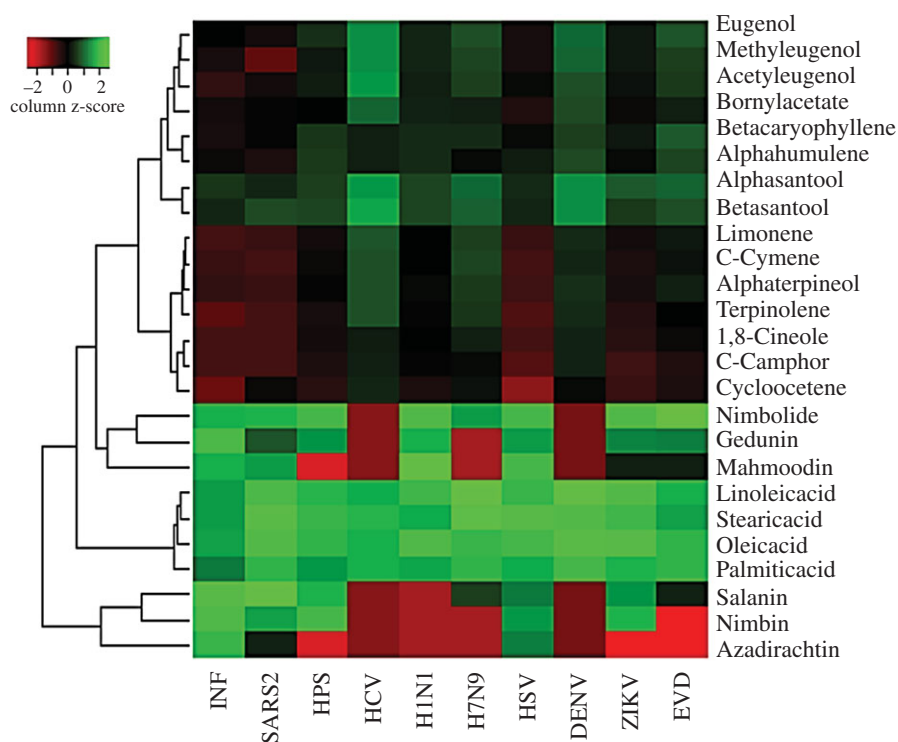
The heat map analysis of constituents (as shown in figure 5) illustrates the molecular binding characteristics of formulation (B) for denaturing the virus's cell wall and/or membrane. Individual docking performance of constituent chemicals as per the high energy of the Ludi algorithm elucidates promising bioactivity of salanin, nimbin, gedunin and mahmoodin for inhibiting the potent effect of influenza A virus. The structural compatibility of the formulation was dominated by pharmacophore of chemical constituents which was more compatible with the active binding sites of influenza A virus. Similarly, molecular docking performance of salanin, stearic acid and oleic acid contribute with mild to moderate binding against the homology modelled envelope protein of SARS-CoV-2. The structural docking was attributed to a combined effect of more hydrogen acceptors and rotation of bonds in aliphatic structures of stearic acid and oleic acid. Furthermore, constituent chemicals of *A. indica*, *S. aromaticum*, *Santalum album* and *Ocimum tenuiflorum* exhibited potent behaviour against the protein-structured cell wall (except glycoprotein of herpes virus). Among herbal-extract major constituents, the bioactivities of stearic acid, linoleic acid, oleic acid, palmitic acid, nimbin and nimbolin were found to be more effective for inhibiting the activity of airborne viruses. Availability of hydrogen bond acceptors in nimbin and nimbolin elevates the extent of molecular docking, whereas aliphatic characteristics and relatively low molecular polar surface areas of oleic acid, linoleic acid, stearic acid and palmitic acid facilitate the structural combability against the protein structures of viruses. The herpes virus wrapping of glycoprotein D was dominated by chemical constituents of *Eucalyptus citriodora* and *S. aromaticum* due to the optimized energy per unit of the Ludi algorithm of eugenol, o-cymene and limonene.

5. Contact angle analysis

The surface wetting analysis of spray-coated C6-fluorocarbon on polypropylene-based non-woven layer against water molecules was investigated using a contact angle goniometer. Fluoro molecule-dispersed solution of C6-fluorocarbon
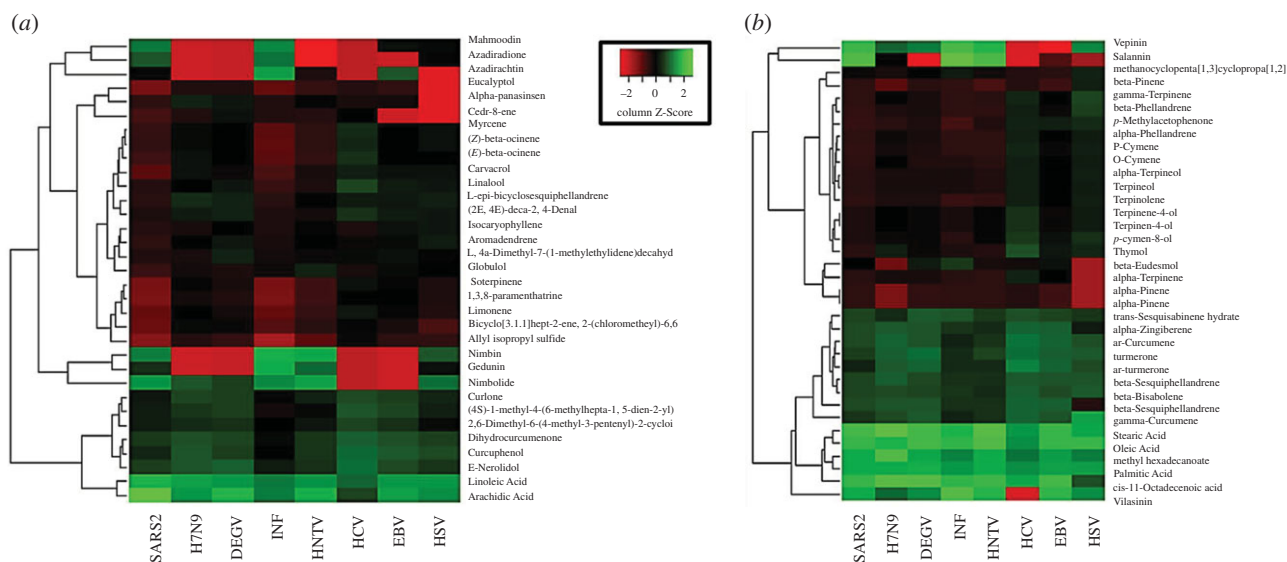
Figure 4. Heat map analysis of major constituent chemicals in the herbal-extract-based formulation (A) against airborne viruses (SARS2, severe respiratory syndrome coronavirus 2; H7N9, drug-resistant influenza A; DEGV, Dengue virus; INF, influenza; HNTV, hantavirus; HCV, hepatitis C virus; EBV, Ebola virus; HSV, herpes simplex virus).


Figure 5. The heat map analysis of major constituent chemicals in the herbal-extract-based formulation (B) against airborne viruses (INF, influenza; SARS2, severe acute respiratory syndrome coronavirus 2; HPS, hantavirus; HCV, hepatitis C virus; DENV, Dengue virus; HSV, herpes simplex virus; ZIKV, Zika virus; EVD, Ebola virus disease).

(TUBIGUARD 30-F) was spray coated [50] on the non-woven material in such a way that it retained the porous structure of the non-woven fabric and formed a thin layer of 0.1 µm on fibre surface. C6-Fluorocarbon includes six carbon-based molecules in its main structure, bonded to different fluorine atoms. CHT Group (from Germany) have demonstrated textile finishing using C6-based fluorocarbon for decreasing the surface energy of spray-coated non-woven surface, for enhancing the water repellency [51–54]. Static contact angle of spray-coated C6-fluorocarbon on polypropylene non-woven layer was found to be $130 \pm 2°$ (outer layer of face mask) and $91.1 \pm$

$2°$, respectively (figure 6a,b). CHT Group further investigated the activity of C6 fluorocarbon for inhibiting the bacterial and viral contamination due to adsorption of aerosol droplets over the exposed layer of the protective mask [54].

6. Conclusion

Present study demonstrated functionalization and utilization of non-woven fabric in a protective face mask for combating the spread of infectious SARS-CoV-2 virus. The developed
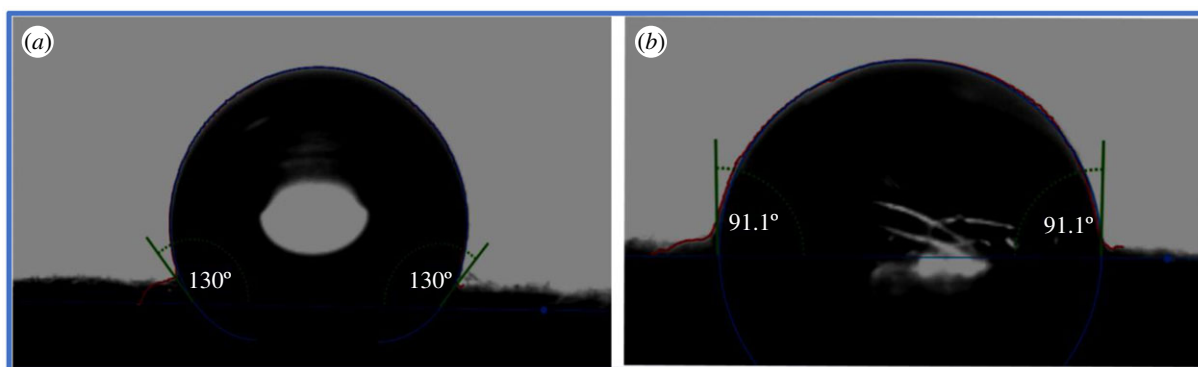
Figure 6. Contact angle analysis of the outer layer of mask material. (*a*) Outer layer in face mask and (*b*) inner side of top layer of face mask.

four-ply face mask demonstrated BFE of 99.65% and the encapsulated herbal extract phytochemicals helped in improving the immune-boosting of mask wearer. Surface functionalization of outer layer by spray coating of TUBIGARD 30F generated hydrophobicity (water contact angle (WCA) of approximately 130°), which facilitated in inhibiting the transmission of aerosol particles from the surrounding air. Fine fibre diameter and compact fabric structure supported in effective blocking of harmful viruses and bacteria. Second layer of face mask consisting of polyester-based melt-blown non-woven filter media helped in inhibiting transmission of aerosol particles of 5 µm in size. Third layer of the face mask containing PLA polymer and herbal phytochemicals helped in enhancing the BFE and giving immune-boosting through inhalation to mask wearer. A thorough computational analysis was performed using Lib-Dock algorithm and showed docking score of herbal phytochemicals against harmful virus structures. Herbal phytochemical constituents such as salanin, arachidic acid, oleic acid, linoleic acid, stearic acid and palmitic acid demonstrated promising results for utilization as immune-boosting agents to inhibiting the viral infections. The developed four-ply face mask was tested against *S. aureus* (as per AATCC 6538 standard) which showed BFE of 99.65%. Further, the developed face mask demonstrated sufficient breathability as per the Indian IS 9734:2002 standard which showed breathing resistance of 30 Pa at aerosol flow rate of $30 \, \mathrm{l \, h^{-1}}$.

7. Material and methods

7.1. Material sourcing

PLA (Fiberel, PLA white, 1.75 mm diameter) was obtained from Rever Industries, Nashik. Dichloromethane (99% pure) was obtained from Thermo Fisher Scientific India Pvt Ltd. Polyester fibre-based melt-blown non-woven fabric (VN 140 GSM) and polypropylene-based spun-bonded non-woven fabric were procured from Venus Safety and Health Pvt Ltd. *A. indica, Eucalyptus citriodora, Santalum album, Cinnamomum camphora, Ocimum tenuiflorum, S. aromaticum* and *C. longa* L. were obtained from Vishal Chemicals, Mumbai. Mask thickness was measured using a digital thickness meter gauge. TUBIGUARD 30-F (C6-fluorocarbon-based dispersion solution) and TUBICOAT FIX H26 (cross-linking agent) were obtained from CHT Group Germany, and the resulting solution was spray-coated using hand-controlled spray gun.

7.2. Spray-coating technique

Spray-coating solution for formulation A was prepared by dissolving PLA (2 wt.% of solution) in dichloromethane solvent under continuous stirring (200 rpm) at room temperature. Herbal extracts containing *A. indica* (2 wt.% of solution), *Eucalyptus citriodora* (1 wt.% of solution) and *C. longa* L. (1 wt.% of solution) were added to the dispersed solution while maintaining continuous stirring. Other spray-coating solution for formulation B was prepared by replacing the herbal extracts to *Azadirachta indica* (1 wt.% of solution), *Santalum album* (0.8 wt.% of solution), *Eucalyptus citriodora* (0.5 wt.% of solution), *Cinnamomum camphora* (0.1 wt.% of solution), *Ocimum tenuiflorum* (0.1 wt.% of solution) and *Syzygium aromaticum* (0.1 wt.% of solution). PLA/herbal-extract solution was spray coated on filter media using a customized spray-coating machine, while maintaining the distance between tip of spray and non-woven fabric as 1 m to get the optimized thickness for effective filtration efficacy.

7.3. Bacterial filtration efficiency and anti-microbial characteristics

BFE of the face mask was evaluated as per ASTM-F2101-19 standard [48,55]. A prepared test specimen was incubated at a temperature of $21 \pm 5°C$ and relative humidity around $85\% \pm 5\%$ for 4 h in order to adapt adequate operating conditions as per described in practice E171/E171M. The bacterial culture was prepared using adequate volume of tryptic soy broth, conditioned at $37 \pm 2°C$ for duration of 24 ± 2 h in the presence of mild shaking conditions. The developed bacterial culture was diluted in peptone water for achieving concentration of $5 \times 10^5 \, \mathrm{CFU \, ml^{-1}}$. The bacterial challenge delivery rate was adjusted to 1700–3000 viable particles per test. The flow rates of the bacterial challenge were monitored using a six-stage viable particle cascade impactor, without any test specimen to evaluate the effectiveness of aerosol particles during the testing. The aerosol particles were directed towards mask material, and the bacterial challenge was delivered to nebulizer using a peristaltic pump and further exposed on the cascade impactor. Mean particle size of the aerosol droplets was adjusted at 3 ± 0.3 µm. The test specimen was mounted on the agar plates and kept in cascade impactor such that outer layer faced the flow of aerosol particles. The aerosol particles were exposed over the test specimen for a duration of 2 min, with flow rate adjusted to $28.3 \, \mathrm{l \, m^{-1}}$. After the completion of positive control of test specimen, agar plates were removed and conditioned at $37 \pm 2°C$ for a time duration of 48 ± 2 h. The negative control was obtained by collecting a sample of air on agar plates from specimen chamber after the duration of 2 min and incubated. The agar plates were counted for bacterial growth, and BFE of the test specimen mask was determined by the following equation:

$$\text{bacterial filtration efficiency (\%)} = \frac{C - T}{C} \times 100, \qquad (7.1)$$

where *C* is total average plate count for test controls and *T* is count for test sample of plate.

7.4. Breathing resistance analysis

Breathability of the face mask was evaluated as per Indian IS 9473:2002 [56] standard; the testing was carried out on the dummy human prototype to analyse the breathing resistance. A breathing resistance of 30 Pa at aerosol flow rate of $30\,l\,h^{-1}$ was reported under standard temperature and pressure conditions. The face mask was conditioned by simulating the wearing treatment by adjusting the breathing machine at 25 cycles min^{-1} and 2 l per stroke. Half filtering mask was affixed on Sheffield dummy head to evaluate the breathing performance. A saturator was placed in the exhalation line adjusted at temperature of 37°C, and saturated air was adjusted at $37 \pm 2°C$ at the mouth interface. The filtering half masks were subjected to thermal cycles at $70 \pm 3°C$ in dry atmosphere and $30 \pm 3°C$ for duration of 24 h, respectively. Further, the test specimen was kept in the enclosure, and the test subject was subjected to walking at a speed of $6\,km\,h^{-1}$ for a duration of 2 min. Concentration of testing agent was measured inside face mask to develop the background level and reading was recorded. The test atmosphere was switched on and the test subject was allowed to walk for 2 min until the test atmosphere was stabilized. At the same time the test subject should keep walking at various facial movements for duration of 10 min. Subsequently, the test atmosphere was turned off, and test agent was cleared from the enclosure.

7.5. Field-emission scanning electron microscopy

Surface morphology of the non-woven protective face mask was investigated by using FE-SEM (Model: FE-SEM, Make: Carl-Zeiss AG, JSM-6700F, Germany). The surface morphology of fine fibre structures in non-woven fabrics was analysed for assessing the compactness in surface area of protective face mask. Surface morphology analysis was important for understanding the filtration characteristics of non-woven layers.

7.6. Contact angle analysis

Surface wetting analysis is important for understanding the interaction of liquid-phased aerosol particles in air with mask material [57]. In the present study, a drop shape analyser (Model: DSA 25E, Make: Kruss GmbH, Germany) was used for the contact angle analysis. WCA was recorded by placing a standard 8 µl drop of deionized water on the surface at room temperature of $25 \pm 2°C$, and the contact angle was measured using Young–Laplace method [15]. WCA was recorded four times, and the final average value was taken as standard.

7.7. Computational analysis of phytochemicals

Computational assessment of two separate formulations A and B (details given in §7.2) of phytochemicals to counter the bacterial and viral protein structures was performed using docking score-functioned LibDock algorithm [58,59]. The algorithm was functioned for docking ligands at active receptor location, supporting ligand configurations to polar and non-polar receptor interactions. Recording of the optimized scoring positions, and the process mainly depends on binding energy, rotation of bonds and structural properties [60]. The docking performance of interactions was improved by Broyden Fletcher Goldfarb Shanno algorithm along with steady force field minimization. Heat map technique was more precise compared to picto-trendline or dot map for determining the spread of infectious bacteria and virus [61]. Proteins and ligands at drug target site were retrieved from protein data-bank (PDB) structure database. Theoretical models of ligand and protein structures were used to record the docking score. Main phytochemical constituents of the therapeutic *Santalum album*, *A. indica*, *Cinnamomum camphora*, *Eucalyptus citriodora*, *Ocimum tenuiflorum*, *S. aromaticum* and *C. longa* L. were sourced from PubChem database. Raw protein structures were obtained from PDB database. Docking analysis was performed to investigate improved binding activity of constituent phytochemicals by insertion of missing atoms in incomplete residues and modelling of missing loop areas, removing alternative conformations, standardizing the atom names and removing destructive steric clashes. The molecular interactions within ligand and receptor were recorded by analysing molecular docking performance, using computer-aided drug design and structural molecular biology.

References

1. Belongia EA, Osterholm MT. 2020 COVID-19 and flu, a perfect storm. *Science* **368**, 1163. (doi:10.1126/science.abd2220)

2. World Health Organization. 2020 Clinincal management of COVID-19.

3. Stelzer-Braid S, Oliver BG, Blazey AJ, Argent E, Newsome TP, Rawlinson WD, Tovey ER. 2009 Exhalation of respiratory viruses by breathing, coughing, and talking. *J. Med. Virol.* **81**, 1674–1679. (doi:10.1002/jmv)

4. Yan J, Grantham M, Pantelic J, Bueno PJ, Mesquita D, Albert B, Liu F. 2017 Infectious virus in exhaled breath of symptomatic seasonal influenza cases from a college community. *Proc. Natl Acad. Sci. USA* **115**, 1081–1086. (doi:10.1073/pnas.1716561115)

5. Bhattacharjee S, Bahl P, Chughtai AA, MacIntyre CR. 2020 Last-resort strategies during mask shortages: optimal design features of cloth masks and decontamination of disposable masks during the COVID-19 pandemic. *BMJ Open*

Res. Res. **7**, 1–10. (doi:10.1136/bmjresp-2020-000698)

6. Ajmeri JR, Ajmeri CJ. 2016 *Developments in nonwoven materials for medical applications*. Amsterdam, The Netherlands: Elsevier Ltd.

7. Ajmeri JR, Ajmeri CJ. 2011 *Nonwoven materials and technologies for medical applications*. Cambridge, UK: Woodhead Publishing Limited. See https://doi.org/10.1533/9780857093691.1.106.

8. Balasubramanian K, Yadav R, Prajith P. 2015 Antibacterial nanofibers of polyoxymethylene/gold

for pro-hygiene applications. *Int. J. Plastics Technol.* **19**, 363–367. (doi:10.1007/s12588-015-9127-y)

9. Yadav R, Kandasubramanian B. 2013 Egg albumin PVA hybrid membranes for antibacterial application. *Mater. Lett.* **110**, 130–133. (doi:10.1016/j.matlet.2013.07.109)

10. Zhu X, Dai Z, Xu K, Zhao Y, Ke Q. 2019 Fabrication of multifunctional filters via online incorporating nano-TiO_2 into spun-bonded/melt-blown nonwovens for air filtration and toluene degradation. *Macromol. Mater. Eng.* **304**, 1900350. (doi:10.1002/mame.201900350)

11. Tellier R. 2006 Review of aerosol transmission of influenza A virus. *Emerg. Infect. Dis.* **12**, 1657–1662. (doi:10.3201/eid1211.060426)

12. MacIntyre CR *et al.* 2009 Face mask use and control of respiratory virus transmission in households. *Emerg. Infect. Dis.* **15**, 233–241. (doi:10.3201/eid1502.081167)

13. Lustig S, Biswakarma JJH, Rana D, Tilford H, Hu W, Su M, Rosenblatt MS. 2020 *Effectiveness of common fabrics To block aqueous aerosols of virus-like nanoparticles.* ACS Nano **14**, 7651–7658. (doi:10.1021/acsnano.0c03972)

14. Choi J, Yang BJ, Bae GN, Jung JH. 2015 Herbal extract incorporated nanofiber fabricated by an electrospinning technique and its application to antimicrobial air filtration. *ACS Appl. Mater. Interfaces* **7**, 25 313–25 320. (doi:10.1021/acsami.5b07441)

15. Patil NA *et al.* 2021 Needleless electrospun phytochemicals encapsulated nanofibre based 3-ply biodegradable mask for combating COVID-19 pandemic. *Chem. Eng. J.* **416**, 129152. (doi:10.1016/j.cej.2021.129152)

16. Kadam V, Bach Y, Schutz J, Louis I, Padhye R, Wang L. 2021 Gelatin/β-cyclodextrin bio-nanofibers as respiratory filter media for filtration of aerosols and volatile organic compounds at low air resistance. *J. Hazard. Mater.* **403**, 123841. (doi:10.1016/j.jhazmat.2020.123841)

17. Liao L, Xiao W, Zhao M, Yu X, Wang H, Wang Q, Chu S, Cui Y. 2020 Can N95 respirators be reused after disinfection? How many times? *ACS Nano* **14**, 6348–6356. (doi:10.1021/acsnano.0c03597)

18. Song B, Xu Q. 2016 Highly hydrophobic and superoleophilic nanofibrous mats with controllable pore sizes for efficient oil/water separation. *Langmuir* **32**, 9960–9966. (doi:10.1021/acs.langmuir.6b02500)

19. Borkotoky S, Banerjee M. 2020 A computational prediction of SARS-CoV-2 structural protein inhibitors from Azadirachta indica (Neem). *J. Biomol. Struct. Dyn.* **39**, 4111–4121. (doi:10.1080/07391102.2020.1774419)

20. Benencia F, Courrèges MC. 1999 Antiviral activity of sandalwood oil against Herpes simplex viruses-1 and -2. *Phytomedicine* **6**, 119–123. (doi:10.1016/S0944-7113(99)80046-4)

21. Yadav R, Balasubramanian K. 2015 Polyacrylonitrile/*Syzygium aromaticum* hierarchical hydrophilic nanocomposite as a carrier for antibacterial drug

22. Xiong X, Wang P, Su K, Cho WC, Xing Y. 2020 Chinese herbal medicine for coronavirus disease 2019: a systematic review and meta-analysis. *Pharmacol. Res.* **160**, 105056. (doi:10.1016/j.phrs.2020.105056)

23. Siemieniuk RAC *et al.* 2020 Drug treatments for covid-19: living systematic review and network meta-analysis. *BMJ* **370**, m2980. (doi:10.1136/bmj.m2980)

24. Bartoňková I, Dvořák Z. 2018 Assessment of endocrine disruption potential of essential oils of culinary herbs and spices involving glucocorticoid, androgen and vitamin D receptors. *Food Funct.* **9**, 2136–2144. (doi:10.1039/c7fo02058a)

25. Kumar A, Kumar P. 2020 Quantitative structure toxicity analysis of ionic liquids toward acetylcholinesterase enzyme using novel QSTR models with index of ideality of correlation and correlation contradiction index. *J. Mol. Liq.* **318**, 114055. (doi:10.1016/j.molliq.2020.114055)

26. Podgórski A, Bałazy A, Gradoń L. 2006 Application of nanofibers to improve the filtration efficiency of the most penetrating aerosol particles in fibrous filters. *Chem. Eng. Sci.* **61**, 6804–6815. (doi:10.1016/j.ces.2006.07.022)

27. Wang Z, Pan Z. 2015 Preparation of hierarchical structured nano-sized/porous poly(lactic acid) composite fibrous membranes for air filtration. *Appl. Surf. Sci.* **356**, 1168–1179. (doi:10.1016/j.apsusc.2015.08.211)

28. Wang Q, Maze B, Tafreshi HV, Pourdeyhimi B. 2006 A case study of simulating submicron aerosol filtration via lightweight spun-bonded filter media. **61**, 4871–4883. (doi:10.1016/j.ces.2006.03.039)

29. Uppal R, Bhat G, Eash C, Akato K. 2013 Meltblown nanofiber media for enhanced quality factor. *Fibers Polym.* **14**, 660–668. (doi:10.1007/s12221-013-0660-z)

30. Zhu J, Bahramian Q, Gibson P, Gibson HS, Sun G. 2012 Chemical and biological decontamination functions of nanofibrous membranes. *J. Mater. Chem.* **22**, 8532–8540. (doi:10.1039/c2jm16605d)

31. Koena Selatile M, Ojijo V, Sadiku R, Sinha S. 2020 Development of bacterial-resistant electrospun polylactide membrane for air filtration application: effects of reduction methods and their loadings. *Polym. Degrad. Stab.* **178**, 109205. (doi:10.1016/j.polymdegradstab.2020.109205)

32. Balasubramanian K, Kodam KM. 2014 Encapsulation of therapeutic lavender oil in an electrolyte assisted polyacrylonitrile nanofibres for antibacterial applications. *RSC Adv.* **4**, 54 892–54 901. (doi:10.1039/c4ra09425e)

33. Akduman C. 2021 Cellulose acetate and polyvinylidene fluoride nanofiber mats for N95 respirators. *J. Ind. Text.* **50**, 1239–1261. (doi:10.1177/1528083719858760)

34. Selatile MK, Ray SS, Ojijo V, Sadiku R. 2018 Depth filtration of airborne agglomerates using electrospun bio-based polylactide membranes.

J. Env. Chem. Eng. **6**, 762–772. (doi:10.1016/j.jece.2017.12.070)

35. Selvam AK, Nallathambi G. 2015 Polyacrylonitrile/silver nanoparticle electrospun nanocomposite matrix for bacterial filtration. **16**, 1327–1335. (doi:10.1007/s12221-015-1327-8)

36. Zhang S, Liu H, Yin X, Li Z, Yu J, Ding B. 2017 Tailoring mechanically robust poly(m-phenylene isophthalamide) nanofiber/nets for ultrathin high-efficiency air filter. *Sci. Rep.* **7**, 40550. (doi:10.1038/srep40550)

37. Qin X, Wang S. 2006 Filtration properties of electrospinning nanofibers. *Appl. Polym. Sci.* **102**, 1285–1290. (doi:10.1002/app.24361)

38. Zhu M *et al.* 2017 Electrospun nanofibers membranes for effective air filtration. *Macromol. Mater. Eng.* **302**, 1600353. (doi:10.1002/mame.201600353)

39. Aydin O, Emon B, Cheng S, Hong L, Chamorro LP. 2020 Performance of fabrics for home-made masks against the spread of COVID-19 through droplets: a quantitative mechanistic study. *Extreme Mech. Lett.* **40**, 100924. (doi:10.1016/j.eml.2020.100924)

40. Zangmeister CD, Radney JG, Vicenzi EP, Weaver JL. 2020 Filtration efficiencies of nanoscale aerosol by cloth mask materials used to slow the spread of SARS CoV-2. *ACS Nano* **14**, 9188–9200. (doi.org/10.1021/acsnano.0c05025)

41. Ali A, Shahid A, Hossain D, Islam N. 2019 Antibacterial bi-layered polyvinyl alcohol (PVA)-chitosan blend nanofibrous mat loaded with Azadirachta indica (neem) extract. *Int. J. Biol. Macromol.* **138**, 13–20. (doi:10.1016/j.ijbiomac.2019.07.015)

42. Subramani K, Murugan V, Shanmugam BK, Rangaraj S, Palanisamy M, Venkatachalam R, Suresh V. 2017 Ecofriendly route to enhance the antibacterial and textural properties of cotton fabrics using herbal nanoparticles from Azadirachta indica (neem). *J. Alloys Compd.* **723**, 698–707. (doi:10.1016/j.jallcom.2017.06.242)

43. Govindaraj P, Kandasubramanian B, Kodam KM. 2014 Molecular interactions and antimicrobial activity of curcumin (Curcuma longa) loaded polyacrylonitrile films. *Mater. Chem. Phys.* **147**, 934–941. (doi:10.1016/j.matchemphys.2014.06.040)

44. Verma V, Balasubramanian K. 2014 Experimental and theoretical investigations of *Lantana camara* oil diffusion from polyacrylonitrile membrane for pulsatile drug delivery system. *Mater. Sci. Eng C* **41**, 292–300. (doi:10.1016/j.msec.2014.04.061)

45. Balasubramanian K, Kodam KM. 2016 Correction: encapsulation of therapeutic lavender oil in an electrolyte assisted polyacrylonitrile nanofibres for antibacterial applications. *RSC Adv.* **6**, 75 420–75 421. (doi:10.1039/C6RA90067D)

46. Kulkarni SA, Nagarajan SK, Ramesh V, Palaniyandi V, Selvam SP, Madhavan T. 2020 Computational evaluation of major components from plant essential oils as potent inhibitors of SARS-CoV-2 spike protein. *J. Mol. Struct.* **1221**, 128823. (doi:10.1016/j.molstruc.2020.128823)

47. Procter & Gamble. 2021 Vicks Inhaler. See https://www.vicks.co.in/en-in/browse-products/decongestion-category/vicks-inhaler (accessed 6 November 2021).

48. Schnecke V, Swanson CA, Getzoff ED, Trainer JA, Kuhn LA. 1998 Screening a peptidyl database for potential ligands to proteins with side-chain flexibility, proteins: structure. *Funct. Genet.* **33**, 74–87. (doi:10.1002/(SICI)1097-0134(19981001)33:1<74::AID-PROT7>3.0.CO;2-L)

49. Zhou L, Wang J, Wang K, Xu J, Zhao J, Shan T, Luo C. 2012 *Secondary metabolites with antinematodal activity from higher plants*. Amsterdam, The Netherlands: Elsevier. See https://doi.org/10.1016/B978-0-444-59514-0.00003-1.

50. Zyschka R. 2020 FACE MASKS, Tübingen.

51. Gavrilenko O, Wang X. 2019 Functionalized nanofibrous coating on cotton fabrics. *Cellulose* **26**, 4175–4190. (doi:10.1007/s10570-019-02342-y)

52. De Smet D, Weydts D, Vanneste M. 2015 Environmentally friendly fabric finishes. In *Sustainable apparel: production, processing and recycling*, 1st edn (ed. R Blackburn), pp. 3–33. New York, NY: Elsevier.

53. Rezić I, Kiš A. 2020 Design of experiment approach to optimize hydrophobic fabric treatments. *Polymers* **12**, 2131. (doi:10.3390/polym12092131)

54. Zyschka R. 2020 FACE MASKS, Tübingen.

55. ASTM F2101. 2019 Standard test method for evaluating the bacterial filtration efficiency (BFE) of medical face mask materials, using a biological aerosol of Staphylococcus aureus 1. *Am. Soc. Testing Mater.* **2019**, 1–5. (doi:10.1520/F2101-19.2)

56. Bureau of Indian Standards. 2014 Respiratory protective devices filtering half masks to protect against particles specification.

57. Gore PM, Kandasubramanian B. 2018 Heterogeneous wettable cotton based superhydrophobic Janus biofabric engineered with PLA/functionalized-organoclay microfibers for efficient oil-water separation.

J. Mater. Chem. A. **6**, 7457–7479. (doi:10.1039/c7ta11260b)

58. Jiang S et al. 2020 Computational study on new natural compound inhibitors of indoleamine 2,3-dioxygenase 1. *Aging* **12,** 11 349–11 363. (doi:10.18632/aging.103113)

59. Jiang L, Zhang X, Chen X, He Y, Qiao L, Zhang Y, Li G, Xiang Y. 2015 Virtual screening and molecular dynamics study of potential negative allosteric modulators of mGluR1 from Chinese herbs. *Molecules* **20**, 12 769–12 786. (doi:10.3390/molecules200712769)

60. Rao SN, Head MS, Kulkarni A, LaLonde JM. 2007 Validation studies of the site-directed docking program LibDock. *J. Chem. Inf. Model.* **47**, 2159–2171. (doi:10.1021/ci6004299)

61. Fagerlin A, Valley TS, Scherer AM, Knaus M, Das E, Zikmund-Fisher BJ. 2017 Communicating infectious disease prevalence through graphics: results from an international survey. *Vaccine* **35**, 4041–4047. (doi:10.1016/j.vaccine.2017.05.048)